SUPPLEMENTARY MATERIALS

Nephrotoxicity of the BRAF-kinase inhibitor Vemurafenib is driven by off-target Ferrochelatase inhibition

Yuntao Bai[1#], Ji Young Kim[1#], Bijay Bisunke[2], Laura A. Jayne[1], Josie A. Silvaroli[1], Michael S. Balzer[3], Megha Gandhi[1], Kevin M. Huang[1], Veronika Sander[4], Jason Prosek[5], Rachel E. Cianciolo[6], Sharyn D. Baker[1], Alex Sparreboom[1], Kenar D. Jhaveri[7], Katalin Susztak[6], Amandeep Bajwa[2], Navjot Singh Pabla[1*]

SUPPLEMENTARY METHODS

Cell culture and reagents. The human renal tubular epithelial cell line, HK-2 cells (CRL-2190) were obtained from American Type Culture Collection (ATCC) and were grown in keratinocyte media (K-SFM) supplemented with 10% fetal bovine serum as described previously. The murine renal tubular epithelial cell line, Boston University mouse proximal tubule cells (BUMPT, clone 306) were generated by Drs. Wilfred Lieberthal and John Schwartz, Boston University School of Medicine, Boston, MA, and were obtained from Dr. Zheng Dong, Augusta University, Augusta, GA). These cells were grown at 37 °C in Dulbecco's modified Eagle's medium with 10% fetal bovine serum as described recently[1]. Cisplatin, vemurafenib and other kinase inhibitors were obtained from Sigma-Aldrich or Selleckchem. MEK kinase kit was obtained from Sigma-Aldrich (CS0490).

Kinase gatekeeper mutants. The protein kinase plasmids (pCMV6-entry backbone and FLAG tagged) were obtained from Origene. The QuikChange II XL Site-Directed Mutagenesis Kit (Agilent) was utilized to generate mutants, according to methods described in our previous studies[2,3]. The mutagenesis primers for generating the gatekeeper mutations were designed with the help of QuikChange primer design program. Successful mutagenesis was confirmed by DNA sequencing. Lipofectamine LTX (Life Technologies) reagent was used for transient transfection of vector, wild type and gatekeeper mutant plasmids in BUMPT cells for 24 hours, followed by vemurafenib treatment and assessment of cellular viability.

Primary murine tubular cell culture. Primary RTECs were isolated from 6-8 weeks old mice using previously well-established methods[1]. Briefly, after euthanasia, kidneys were removed and renal cortical tissues were minced and digested with 0.75 mg/ml collagenase IV (Thermo-Fisher Scientific). After enzymatic tissue dissociation, cells were centrifuged at 2000 g for 10 min in DMEM/F-12 medium with 32% Percoll (Amersham). Subsequently, the pellets were rinsed with serum-free media and cells were cultured in DMEM/F-12 medium supplemented with 5 µg/ml

transferrin, 5 µg/ml insulin, 0.05 µM hydrocortisone, and 50 µM vitamin C on collagen-coated dishes. Approximately one week later on reaching full confluency, the cells were trypsinized and plated at 1×10^5 cells per well in 24-well plates for subsequent experiments. For *in vitro* Braf gene deletion, primary cells from Braf floxed mice were transduced with high-titer (1×10^8 CFU/ml) LV-CMV-Cre-GFP lentivirus (Kerafast), followed by confirmation by immunoblot analysis at 48 hours. For cell viability and drug treatment experiments, primary RTECs were incubated with 50 µM vemurafenib or vehicle (DMSO) in fresh culture medium for 48 h, followed by viability (trypan blue and MTT) and caspase assays.

Cell viability and caspase assays. For the assessment of cellular viability, we utilized trypan blue staining, MTT, and caspase assays as reported in our previous studies[1]. Transformed RTEC cells lines (BUMPT and HK-2 cells) or primary tubular epithelial cells were plated in 6-well, 24-well, or 96-well plates, followed by treated with appropriate vehicles, cisplatin, vemurafenib, and other kinase inhibitors for 24–48 h. For trypan blue staining, cells from 6-well plates were harvested, followed by trypan blue staining and manual cell counting with a hemocytometer and/or by using Countess Automated Cell Counter (Thermo Fisher). We considered translucent cells as viable and blue-stained cells were considered as non-viable. Finally, cellular viability was estimated by taking the ratio of number of viable cells by the total cell number. In similar experiments where cells were plated in 96-well plates, subsequent to drug treatment, 10 µL of MTT reagent (5 mg/mL MTT in PBS) was added to each well, followed by incubation at 37 °C with 5% CO2 for 4 h. Then, 100 µl of acidified isopropanol (Sigma-Aldrich) was added to each well and absorbance was measured at 590 nm. In certain experiments, IC50 (half-maximal inhibitory concentration) was calculated by nonlinear regression analysis using GraphPad Prism. For measurement of caspase activation as a readout of the extent of cell death, cells grown in 6 well plates were lysed in a buffer containing 1% Triton X-100 to extract cytosolic proteins. 10 µg cell lysates were then added to a caspase assay buffer containing 50 µM DEVD-AFC for 60 min at

37 °C. Fluorescence readings at excitation 360 nm/emission 535 nm was measured, and free AFC standard curve was used to convert the fluorescence reading from the enzymatic reaction into the nM AFC liberated per mg protein per hour as described recently.

Viral Transduction and CRISPR/Cas9 mediated gene deletion. Lentiviral transductions were performed using previously described methods[4]. For Cre-mediated gene excision, cultured primary tubular cells were transduced with high-titer (1×10^8 CFU/ml) LV-CMV-Cre-GFP lentivirus (Kerafast), followed by vemurafenib treatment 48 h later. Braf and FECH gene deletion was carried out in HK-2 cells using Lenti-X™ CRISPR/Cas9 System and Lenti-X Tet-On 3G CRISPR-Cas9 System (Takara Bio), followed by isolation of stable cells. Gene knockout was confirmed by DNA sequencing.

Mice strains and breeding. All animals were handled, and procedures were performed in accordance with the animal use protocol approved by the Institutional Animal Care and Use Committee of the Ohio State University and the University of Tennessee Health Science Center. C57BL/6J, Braf floxed (129S1/SvImJ), Fech mutant (BALB/cJ) and Ggt1-Cre (C57BL/6J) transgenic mice (stock numbers 000664, 006373, 002662, and 012841 respectively) were obtained from Jackson Laboratories. Braf floxed mice were bred with Ggt1-Cre transgenic mice to generate RTEC-specific knockout mice. The Fech mutant mice have been described and characterized previously[5]. These mice were originally generated through an ENU mutagenesis experiment and were found to harbor a Fech loss-of-function single amino acid substitution mutation (M98K). We bred the heterozygous mutant mice with wild type mice to obtain littermate wild type and heterozygous mice. The pups were ear tagged and genotyped at 3 weeks of age using standard PCR-based methods as described recently[1]. The mT/mG mice that express cell membrane-targeted, two-color fluorescent Cre-reporter allele were obtained from Jackson Laboratories (stock no. 007676, on C57BL/6J background) and crossed with GGT-Cre mice. In all the experiments, littermate controls were used.

Cisplatin and Ischemia-reperfusion associated kidney injury. For cisplatin nephrotoxicity experiments, 30 mg/kg cisplatin or vehicle (normal saline) was administered by a single intra peritoneal injection as described previously[6,7]. Subsequently, blood was collected on days 0-2 by submandibular vein bleed and via cardiac puncture after carbon dioxide asphyxiation on day 3. To induce bilateral renal ischemia-reperfusion associated AKI, C57BL/6 mice were administered with ketamine (120 mg/kg, i.p.), xylazine (12 mg/kg, i.p.), and buprenorphine (0.15 mg/kg, s.c.) and placed on a warm pad to maintain the body temperature at 34.5–36°C during surgery. Bilateral flank incision was carried out and the renal vessels on both sides were cross-clamped (26 min ischemia followed by 24 h reperfusion). The Sham mice underwent the same procedure except for vessel clamping as described previously[8,9].

Vemurafenib nephrotoxicity. As described previously[10], vemurafenib was dissolved in an aqueous vehicle containing 2% Klucel LF and adjusted to pH 4 with diluted HCl. Vehicle control and vemurafenib were administered orally (0.2 mL per animal, b.i.d., 8 hours apart) at 20 mg/kg dose for 20 days. Subsequently, blood was collected on days 0-19 by submandibular vein bleed for blood urea nitrogen measurement. At endpoint, blood was collected by via cardiac puncture after carbon dioxide asphyxiation and renal tissues were collected for further examination. For hydrodynamic injection, control (non-specific) or FECH targeting siRNAs from Ambion (25 µg in 0.5 ml of PBS; Austin, TX) or 0.5 ml of PBS was injected into the tail vein as described previously[11,12]. For cobimetinib and vemurafenib combination studies, 5 mg/kg cobimetinib (p.o., q.d) was administered along with 20 mg/kg vemurafenib (p.o., b.i.d) for 15-20 days.

Assessment of renal damage. We assessed functional renal impairment and damage through biochemical (blood urea nitrogen and creatinine) and histological analysis (H&E staining). For biochemical analysis, blood urea nitrogen and creatinine measurement were carried out using QuantiChromTM Urea Assay Kit (DIUR-100) and enzymatic assay-based creatinine measurement (ab65340, Abcam). For histological analysis of renal damage, harvested kidneys

were embedded in paraffin and tissue sections (4 μm) were stained with hematoxylin and eosin by previously described methods. For histopathologic scoring, ten consecutive 100x fields per section from at least three mice per group were examined by an investigator in a blinded fashion. The gradation of tissue damage was scored based on the percentage of damaged tubules as described in our previous studies: 0: no damage; 1: <25%; 2: 25–50%; 3: 50–75%; 4: >75%. Tubules that showed dilation, epithelial flattening, cast formation, loss of brush border and nuclei, and denudation of the basement membrane were considered as damaged.

Vemurafenib pharmacokinetic analysis. Pharmacokinetic studies were performed as previously described[13]. Briefly, 8-12 weeks old C57BL/6 mice male mice were administered with 20 mg/kg vemurafenib. Blood samples were collected at various time intervals via submandibular and retro-orbital bleeds, or cardiac puncture into heparin-coated capillaries or tubes. The blood was spun at 12,000 g for 5 minutes to collect plasma. The plasma was stored at -80C until further bioanalytical quantification. The LCMS/MS system consisted of a Vanquish UHPLC system, a TSQ Quantum Ultra triple quadrupole mass spectrometer from Thermo Fisher Scientific, and Thermo Trace Finder General Quan system software (version 3.3). An Accucore Vanquish C18 column (100 × 2.1 mm, dp = 1.5μm, Thermo Fisher Scientific) was protected by a corresponding XBridge®BEH C18, 5-μm guard column. The injection volume of sample was 5.0 μL. The temperature of the autosampler rack was 4°C, and the temperature of the column was maintained at 40°C. Mobile phase A consisted of water with 0.1% (v/v) formic acid and mobile phase B consisted of acetonitrile: methanol (1:3) with 0.1% (v/v) formic acid. The total run time was 5 min. The optimized gradient 1 started at 0-0.5 min with 10% B; 0.5 - 3.0 min, 95% B; 3.0 - 4.0 min, 95% B; 4.0 - 4.1 min, 10% B; 4.1 - 5.0 min, 10% B with a flow rate of 0.4 mL/min. The MS assay setting with the positive voltage applied to the ESI capillary was set at 3500 V, and the capillary temperature was 342°C with a vaporizer temperature of 358°C. Argon was used as the collision gas at a pressure of 1.5 mTorr. Precursor molecular ions and product ions were recorded for

confirmation and detection of vemurafenib (490.118 > 254.929; >99% purity, Sigma-Aldrich Woburn, MA), using palbociclib as an internal standard (448.268 > 380.111; >99% purity, Alsachim, North York, ON, Canada). Results from assay validation studies involving quality control samples analyzed over several days revealed that the within-day precision and between-day precision ranged 2.88% - 14.5%, with an average accuracy ranging 105% - 114%. The lower limit of quantification was 5 ng/mL.

qPCR analysis. Quantitative polymerase chain reaction (qPCR) was performed for gene expression analysis as described in our previous work[14]. Briefly, one µg RNA from RTECs or renal cortical tissues was reversed transcribed using RevertAid First Strand cDNA Synthesis Kit (Thermo-Fisher Scientific) and qRT-PCR was run using the QuantStudio 7 Flex Real-Time PCR System (Thermo-Fisher Scientific) using SYBR green master mix and gene-specific primers (Sigma). β-actin was used as the internal control and gene expression levels were determined by the comparative CT ($\Delta\Delta^{CT}$) method.

Immunoblot analysis. We prepared whole cell lysates from renal tissues and *in vitro* cultured RTECs using a modified RIPA buffer (20 mM Tris-HCl (pH 7.5), 150 mM NaCl, 1 mM Na2EDTA, 1 mM EGTA, 1% NP-40, 2.5 mM sodium pyrophosphate, 1 mM beta-glycerophosphate, protease, and phosphatase inhibitors) supplemented with 1% SDS. Following protein estimation, 20-75 µg protein per sample was loaded on Invitrogen Bis-tris gradient midi-gels, followed by transfer to PVDF membranes, incubation with primary and secondary antibodies and signal detection by ECL reagent (Cell Signaling). Primary antibodies used for immunoblot analysis were from Santa Cruz Biotech: Fech (377377), GFP (9996) and β-actin (47778), Novus: tdTomato (NBP2-78135), and ECM Bioscience: Braf (RP2011) and were used at 1:1,000 dilution. Secondary anti-rabbit and anti-mouse HRP-conjugated antibodies were from Jackson Immuno-research and were used at 1:2,000 dilutions. Uncropped images of immunoblots are provided in **Supplementary Figure**

18. Using previously described methods[15], densitometric analysis was carried out with Image J software, and the signals of target protein was normalized to β-actin signal of the same sample.

Braf kinase assay. In vitro cultured RTECs or murine renal tissues were lysed with a buffer containing 150 mM NaCl, 1 mM EDTA, 1 mM EGTA, 1% (vol/vol) Triton X-100, 2.5 mM sodium pyrophosphate, 1 mM β-glycerol phosphate, 0.2% (wt/vol) dodecyl β-D-maltoside, and 20 mM Tris (pH 7.5) and supplemented with protease and phosphate inhibitors. These cellular and tissue lysates were then subjected to Braf immunoprecipitation as described in our previous studies. To this end, 1000 µg of protein lysate was incubated with 2.5 µg of IgG (control) or anti-Braf antibody at 4 ^{o}C overnight, followed by addition of 50 µl of agarose protein A/G beads for 4 hours. Bead-bound immunoprecipitates were then collected by centrifugation and washed with lysis buffer four times. Finally, the beads were added to a protein kinase reaction buffer containing 20 µM ATP and myelin basic protein (Millipore) as substrate and incubated at 30 °C for 30 min. Using recently described methods[1] employing the ADP-Glo™ Kinase Assay (Promega) kit, we measured the Braf kinase activity. This assay is a luminescent detection method that provides a measure of relative kinase activity by quantifying the amount of ADP produced during a kinase reaction. To quantify the level of inmmunoprecipiated Braf protein in each sample, immunoblot analysis was performed after the termination of kinase reaction. Relative kinase activity was subsequently calculated by normalizing the kinase activity (luminescence) to the amount of immunoprecipitated Braf protein. Undetectable activity in the renal tissues of $Braf^{PT-/-}$ mice confirmed the specificity of the immunoprecipitation-based kinase assay.

Isolation of GFP positive RTECs. As reported recently[4], mT/mG mice that express cell membrane-targeted, two-color fluorescent Cre-reporter allele were obtained from Jackson Laboratories (stock no. 007676) and crossed with Ggt1-Cre mice. In these transgenic mice prior to Cre recombination, cell membrane-localized tdTomato (mT) is expressed in all the cells/tissues, and Cre recombinase expression induces cell membrane-localized EGFP (mG) fluorescence

expression replacing the red fluorescence. We have thoroughly characterized these mice previously[4] and have shown RTEC-specific GFP expression. For cell isolation, following experimental endpoints, mice were euthanized, kidneys were excised and cortical regions were minced and treated with collagenase, followed passage through 100 µm and 35 µm mesh to generate single cell population. Anti-GFP antibody and MACS columns (Miltenyi Biotech) were used to isolate GFP-positive tubular epithelial cells and GFP-negative cells. The purity (generally greater than 95%) of GFP positive and negative cells was verified by flow cytometric analysis. Western blot analysis of RTEC specific (GFP and SLC22A2) and other cell markers (tdTomato) was also performed as shown in Figure 5D.

Ferrochelatase assay. FECH activity was measured by enzymatic formation of zinc-protoporphyrin IX (Zn-PpIX) using a previously described method[16]. Briefly, cell lysates from cultured cells or renal cortical tissues were incubated with 200 µM PpIX (Sigma) in an 200 µl assay buffer (0.1 M Tris-HCl, 1 mM palmitic acid and 0.3% v/v Tween 20, pH 8.0), followed by addition of 50 µL of 2 mM zinc acetate solution. The reaction mixture was incubated at 37°C followed by addition of 500 µL ice-cold termination buffer (1 mM ethylenediaminetetraaceticacid (EDTA) in 30:70 DMSO/methanol). Susequently, the reaction mixture was centrifuged at 14,000 g for 10 min and the Zn-PpIX in the supernatant was measured with a synergy fluorescence plate reader using a 405 nm excitation/590 nm emission filter. For each sample, a heat-inactivated group was included as a negative control. The specificity of the assay was confirmed using Fech mutant tissues.

Intracellular Heme measurement. For determination of total heme levels, frozen cells were thawed and homogenized in 1%Triton-X100 in TBS and centrifuged at 5,000 × g for 10 minutes to remove debris. Protein concentration was quantified by BCA assay (Pierce, IL) and heme was quantified based on a previously described method[17]. Herein, equal amounts of proteins from different samples were mixed with 2 M oxalic acid and heated at 95°C for 30 minutes to release

iron from heme and generate fluorescent protoporphyrin IX. These samples were then centrifuged at 1,000 × g at 4°C for 10 minutes followed by assessment of fluorescence of the supernatant at 405 nm / 600 nm using a fluorescence microplate reader. These readings were then normalized to protein concentration for each sample. For the same samples, determination of unsaturated protoporphyrin IX levels was carried out. To this end, incubation and heating with oxalic acid steps were omitted. In its place, samples were diluted in PBS, followed by fluorescence measurement and normalization to protein content.

Seahorse Flux Bioanalyzer. BUMPT cells were transferred to a Seahorse 24-well tissue culture plates, and oxygen consumption rate (OCR) was measured, and parameters were calculated as previously described[18]. After measuring basal respiratory rate, oligomycin (Sigma; 2 μM), FCCP (Sigma; 1.5 μM; carbonyl cyanide 4-(trifluoromethoxy)-phenylhydrazone (FCCP)), and electron transport chain (complex I and III) inhibitors, rotenone (Sigma; 0.5 μM), and antimycin A (Sigma; 0.5 μM)) were injected sequentially during the assay. Basal mitochondrial respiration, ATP-linked respiration, proton leak (non-ATP linked oxygen consumption), maximal respiration, non-mitochondrial respiration, reserve respiratory capacity, respiratory control ratio, and coupling efficiency were determined in whole cells according to a previously described procedure[19]. We used, N = 4–5 wells for each experimental group and experiments were repeated a minimum of three times.

Statistical Analysis. In the current study, data in all the graphs are presented as mean with s.d. We used GraphPad Prism software for statistical analysis. $p<0.05$ was considered as statistically significant. To evaluate statistical significance between two groups, two-tailed unpaired Student's t test was performed. For comparisons among three or more groups, one-way ANOVA followed by Tukey's or Dunnett's multiple-comparison test was performed. For statistical analysis of renal damage non-parametric Mann–Whitney U test was used. All experiments were repeated at least three times and no sample outliers were excluded.

Supplementary References

1. Kim JY, Bai Y, Jayne LA, et al. A kinome-wide screen identifies a CDKL5-SOX9 regulatory axis in epithelial cell death and kidney injury. *Nat Commun*. 2020;11(1):1924. doi:10.1038/s41467-020-15638-6

2. Sprowl JA, Ong SS, Gibson AA, et al. A phosphotyrosine switch regulates organic cation transporters. *Nat Commun*. 2016;7:10880. doi:10.1038/ncomms10880

3. van Oosterwijk JG, Buelow DR, Drenberg CD, et al. Hypoxia-induced upregulation of BMX kinase mediates therapeutic resistance in acute myeloid leukemia. *J Clin Invest*. 2018;128(1):369-380. doi:10.1172/JCI91893

4. Kim JY, Bai Y, Jayne LA, et al. A kinome-wide screen identifies a CDKL5-SOX9 regulatory axis in epithelial cell death and kidney injury. *Nat Commun*. 2020;11(1):1924. doi:10.1038/s41467-020-15638-6

5. Bloomer J, Bruzzone C, Zhu L, Scarlett Y, Magness S, Brenner D. Molecular defects in ferrochelatase in patients with protoporphyria requiring liver transplantation. *J Clin Invest*. 1998;102(1):107-114. doi:10.1172/JCI1347

6. Pabla N, Dong G, Jiang M, et al. Inhibition of PKCδ reduces cisplatin-induced nephrotoxicity without blocking chemotherapeutic efficacy in mouse models of cancer. *J Clin Invest*. 2011;121(7):2709-2722. doi:10.1172/JCI45586

7. Pabla N, Gibson AA, Buege M, et al. Mitigation of acute kidney injury by cell-cycle inhibitors that suppress both CDK4/6 and OCT2 functions. *Proc Natl Acad Sci USA*. 2015;112(16):5231-5236. doi:10.1073/pnas.1424313112

8. Bajwa A, Huang L, Kurmaeva E, et al. Sphingosine Kinase 2 Deficiency Attenuates Kidney Fibrosis via IFN-γ. *J Am Soc Nephrol*. 2017;28(4):1145-1161. doi:10.1681/ASN.2016030306

9. Rousselle TV, Kuscu C, Kuscu C, et al. FTY720 Regulates Mitochondria Biogenesis in Dendritic Cells to Prevent Kidney Ischemic Reperfusion Injury. *Front Immunol*. 2020;11:1278. doi:10.3389/fimmu.2020.01278

10. Yang H, Higgins B, Kolinsky K, et al. Antitumor Activity of BRAF Inhibitor Vemurafenib in Preclinical Models of BRAF-Mutant Colorectal Cancer. *Cancer Res*. 2012;72(3):779-789. doi:10.1158/0008-5472.CAN-11-2941

11. Sprowl JA, Ong SS, Gibson AA, et al. A phosphotyrosine switch regulates organic cation transporters. *Nat Commun*. 2016;7:10880. doi:10.1038/ncomms10880

12. Kim JY, Jayne LA, Bai Y, et al. Ribociclib mitigates cisplatin-associated kidney injury through retinoblastoma-1 dependent mechanisms. *Biochem Pharmacol*. 2020;177:113939. doi:10.1016/j.bcp.2020.113939

13. Leblanc AF, Huang KM, Uddin ME, Anderson JT, Chen M, Hu S. Murine Pharmacokinetic Studies. *Bio Protoc*. 2018;8(20). doi:10.21769/BioProtoc.3056

14. Kim JY, Bai Y, Jayne LA, et al. SOX9 promotes stress-responsive transcription of VGF nerve growth factor inducible gene in renal tubular epithelial cells. *J Biol Chem*. 2020;295(48):16328-16341. doi:10.1074/jbc.RA120.015110

15. Pabla N, Bhatt K, Dong Z. Checkpoint kinase 1 (Chk1)-short is a splice variant and endogenous inhibitor of Chk1 that regulates cell cycle and DNA damage checkpoints. *Proc Natl Acad Sci USA*. 2012;109(1):197-202. doi:10.1073/pnas.1104767109

16. Yoshioka E, Chelakkot VS, Licursi M, et al. Enhancement of Cancer-Specific Protoporphyrin IX Fluorescence by Targeting Oncogenic Ras/MEK Pathway. *Theranostics*. 2018;8(8):2134-2146. doi:10.7150/thno.22641

17. Khechaduri A, Bayeva M, Chang H-C, Ardehali H. Heme Levels are Increased in Human Failing Hearts. *J Am Coll Cardiol*. 2013;61(18):1884-1893. doi:10.1016/j.jacc.2013.02.012

18. Namwanje M, Bisunke B, Rousselle TV, et al. Rapamycin Alternatively Modifies Mitochondrial Dynamics in Dendritic Cells to Reduce Kidney Ischemic Reperfusion Injury. *Int J Mol Sci*. 2021;22(10):5386. doi:10.3390/ijms22105386

19. Brand MD, Nicholls DG. Assessing mitochondrial dysfunction in cells. *Biochem J*. 2011;435(2):297-312. doi:10.1042/BJ20110162

Suppl. Figure 1

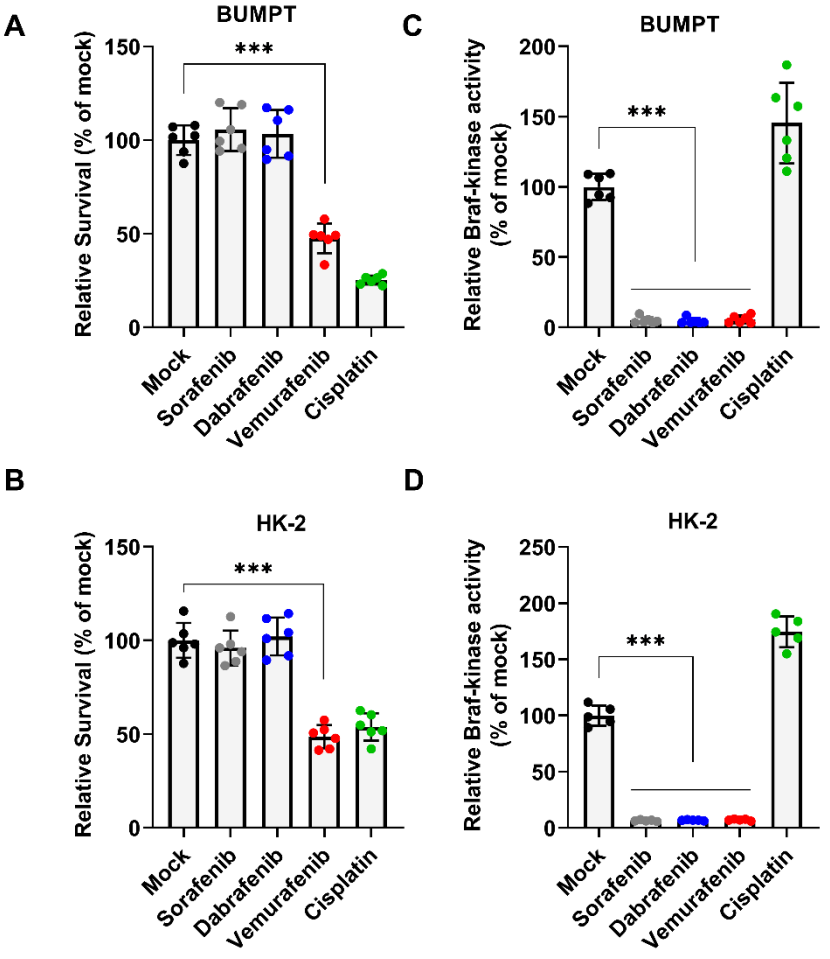

Suppl. Figure 1: Braf-inhibition and *Vemurafenib induced RTEC cell death.* BUMPT and HK-2 cells were treated with vehicle or indicated drugs at 50 µM concentration for 48 hours, followed by assessment of (**A-B**) cellular viability by MTT assays and (**C-D**) in vitro Braf kinase assay. For in vitro kinase assays, Braf was immunoprecipitated from whole cell lysates and the kinase activity was normalized to the amount of immunoprecipitated protein. The data indicates that while sorafenib, dabrafenib, and vemurafenib can inhibit Braf kinase activity, only vemurafenib induces cell death in BUMPT and HK-2 cells. In all the graphs (n=5-6 biologically independent samples), experimental values are presented as mean ± s.d. The height of error bar = 1 s.d. and $p < 0.05$ was indicated as statistically significant. One-way ANOVA followed by Dunnett's was carried out and statistical significance is indicated by *$p < 0.05$, **$p < 0.01$, ***$p < 0.001$.

Suppl. Figure 2

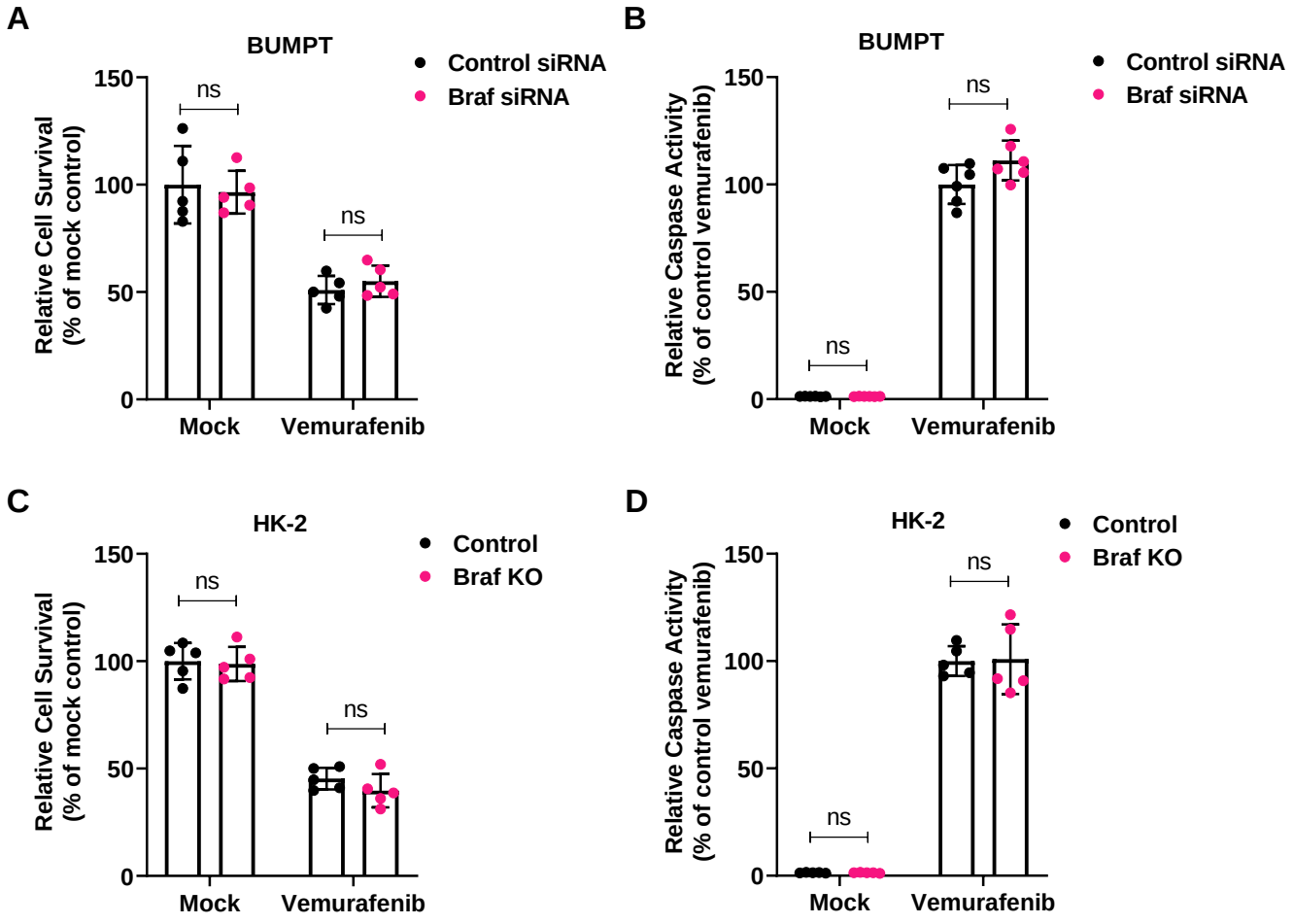

Suppl. Figure 2: ***Vemurafenib induced RTEC cell death is Braf independent.*** (**A-B**) RNAi mediated Braf knockdown in BUMPT cells did not influence vemurafenib associated cell death (50 µM for 48 hours) as assessed by MTT based viability assay and caspase activity measurements. (**C-D**) CRISPR/Cas9 mediated Braf knockout in HK-2 cells did not influence vemurafenib associated cell death (50 µM for 48 hours) as evaluated by MTT based viability assay and caspase activity measurements. In all the graphs (n=5 biologically independent samples), experimental values are presented as mean ± s.d. The height of error bar = 1 s.d. and $p < 0.05$ was indicated as statistically significant. One-way ANOVA followed by Dunnett's was carried out and statistical significance is indicated by *p < 0.05, **p < 0.01, ***p < 0.001.

Suppl. Figure 3

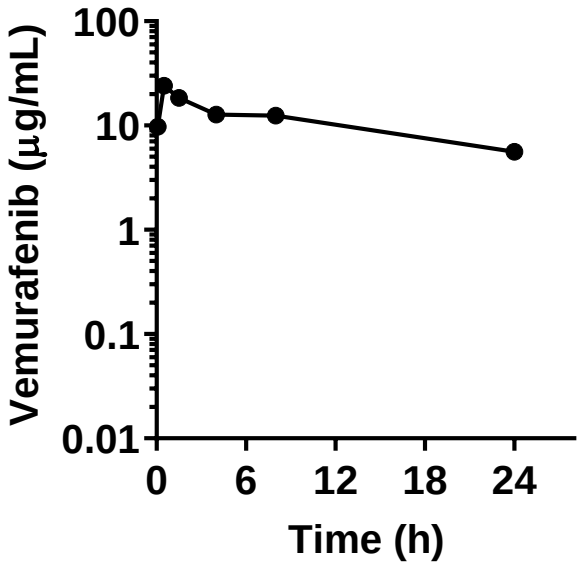

Suppl. Figure 3: ***Vemurafenib pharmacokinetic analysis.*** Age-matched, 8-12 weeks old male C57BL/6J mice were injected with 20 mg/kg vemurafenib followed by pharmacokinetic analysis of vemurafenib levels in the plasma.

Suppl. Figure 4

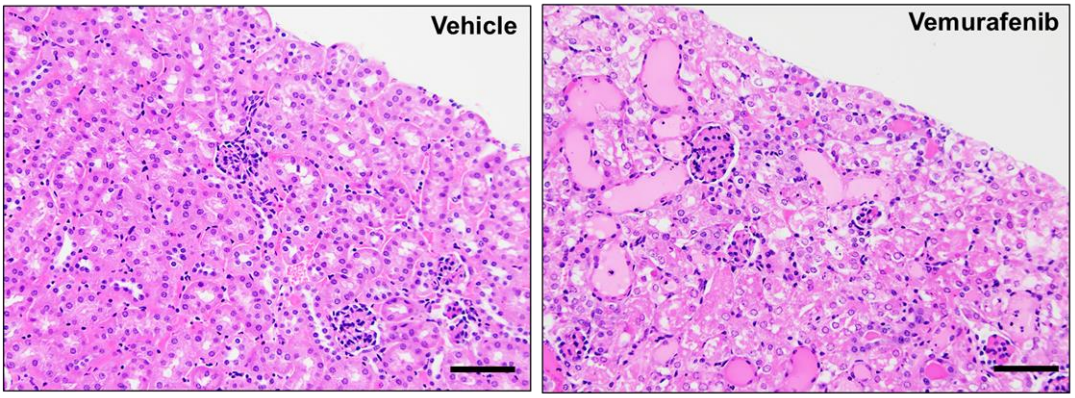

Group	Glomerular necrosis or GN	Dilation of Bowman's capsule	Cortical tubular dilation	Cortical ATN	Cortical Regeneration	Medulla dilation	Medulla ATN	Medulla Regeneration	Casts	Interstitial hemorrhage
Vehicle	-	-	-	-	-	-	-	-	-	-
Vemurafenib	-	-	+	++	-	-	-	-	+, protein and cell	-

Suppl. Figure 4: ***Histopathological analysis of vemurafenib nephrotoxicity*****.** Age-matched, 8-12 weeks old male C57BL/6J mice were treated with either vehicle or 20 mg/kg vemurafenib (p.o, b.i.d.) for 15 days followed by assessment of renal histology (H&E staining). The upper panel shows a representative image depicting tubular injury and necrosis in the vemurafenib group. The lower panel shows the detailed histological analysis of renal tissues from vehicle and vemurafenib treated groups. Overall, tubular injury and cell death was found to be the major histopathological lesion.

Suppl. Figure 5

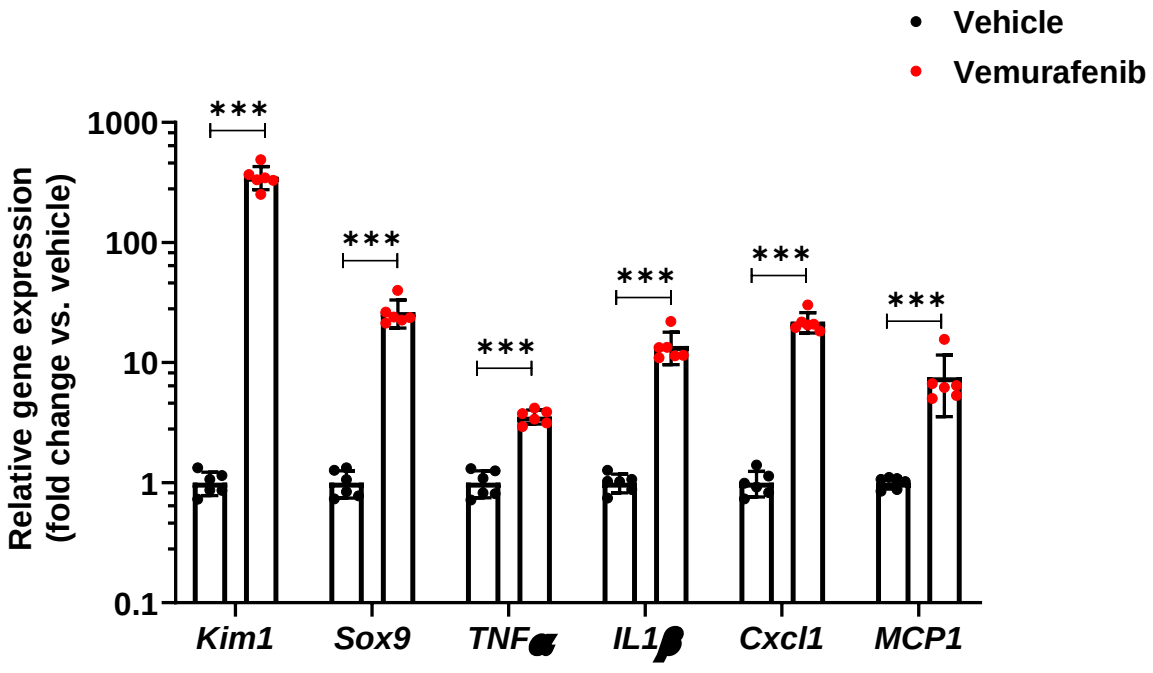

Suppl. Figure 5: Renal gene expression analysis during *vemurafenib nephrotoxicity.* Age-matched, 8-12 weeks old male C57BL/6J mice were treated with either vehicle or 20 mg/kg vemurafenib (p.o, b.i.d.) for 15 days followed by gene expression analysis of indicated genes in renal cortical tissues. Injury, inflammation, and repair related genes were upregulated during vemurafenib nephrotoxicity. In all the bar graphs (n=6 biologically independent samples), experimental values are presented as mean ± s.d. The height of error bar = 1 s.d. and $p < 0.05$ was indicated as statistically significant. Student's t-test was carried out and statistical significance is indicated by *p < 0.05, **p < 0.01, ***p < 0.001.

Suppl. Figure 6

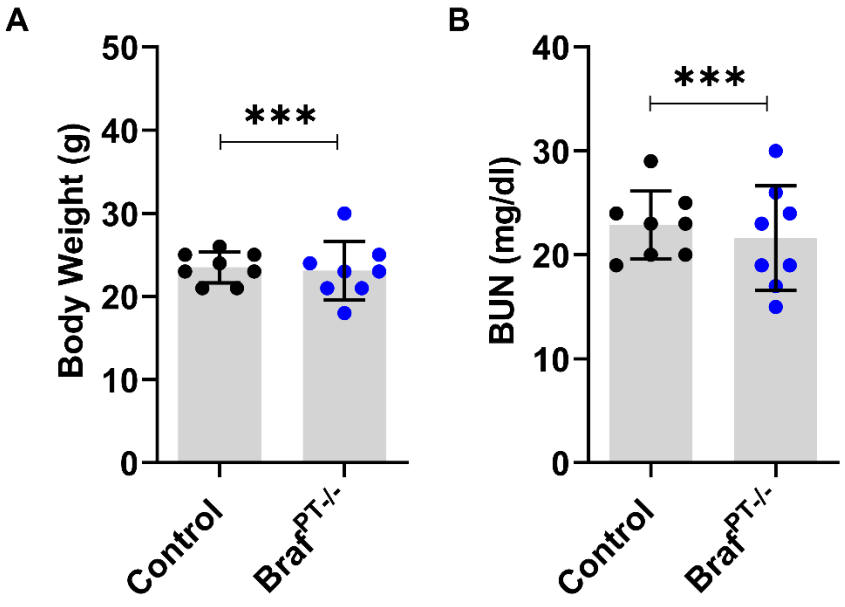

Suppl. Figure 6: ***Effect of Braf gene knockout on renal function***. Littermate control and Braf conditional knockout mice (indicated by $Braf^{PT-/-}$) of 8-12 weeks age had similar (**A**) Body weight and (**B**) Blood urea nitrogen levels, indicating that RTEC-specific Braf gene deletion does not influence renal function under normal baseline conditions. In all the bar graphs (n=8 biologically independent samples), experimental values are presented as mean ± s.d. The height of error bar = 1 s.d. and $p < 0.05$ was indicated as statistically significant. Student's t-test was carried out and statistical significance is indicated by *p < 0.05, **p < 0.01, ***p < 0.001.

Suppl. Figure 7

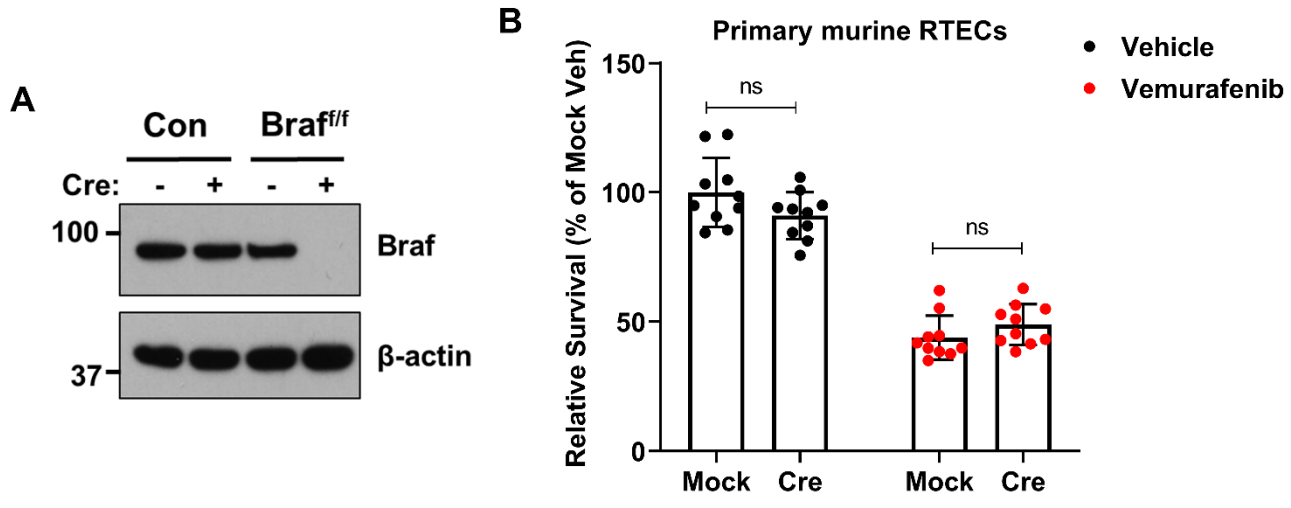

Suppl. Figure 7: ***In vitro Braf gene deletion does not influence vemurafenib associated RTEC cell death***. Primary renal tubular cells were cultured from control and Braf-floxed mice. One week later, lentiviral transductions (Cre) were carried out to delete Braf gene. (**A**) Immunoblot analysis confirmed Braf deletion. Blots are representative of two independent experiments. **(B)** Primary renal tubular cells from Braf-floxed mice with or without Cre transduction were treated with 50 µM vemurafenib, followed by cell viability assessment at 48 hours using trypan blue staining. In all the graphs (n=10 biologically independent samples), experimental values are presented as mean ± s.d. The height of error bar = 1 s.d. and $p < 0.05$ was indicated as statistically significant. One-way ANOVA followed by Dunnett's was carried out and statistical significance is indicated by *$p < 0.05$, **$p < 0.01$, ***$p < 0.001$.

Suppl. Figure 8

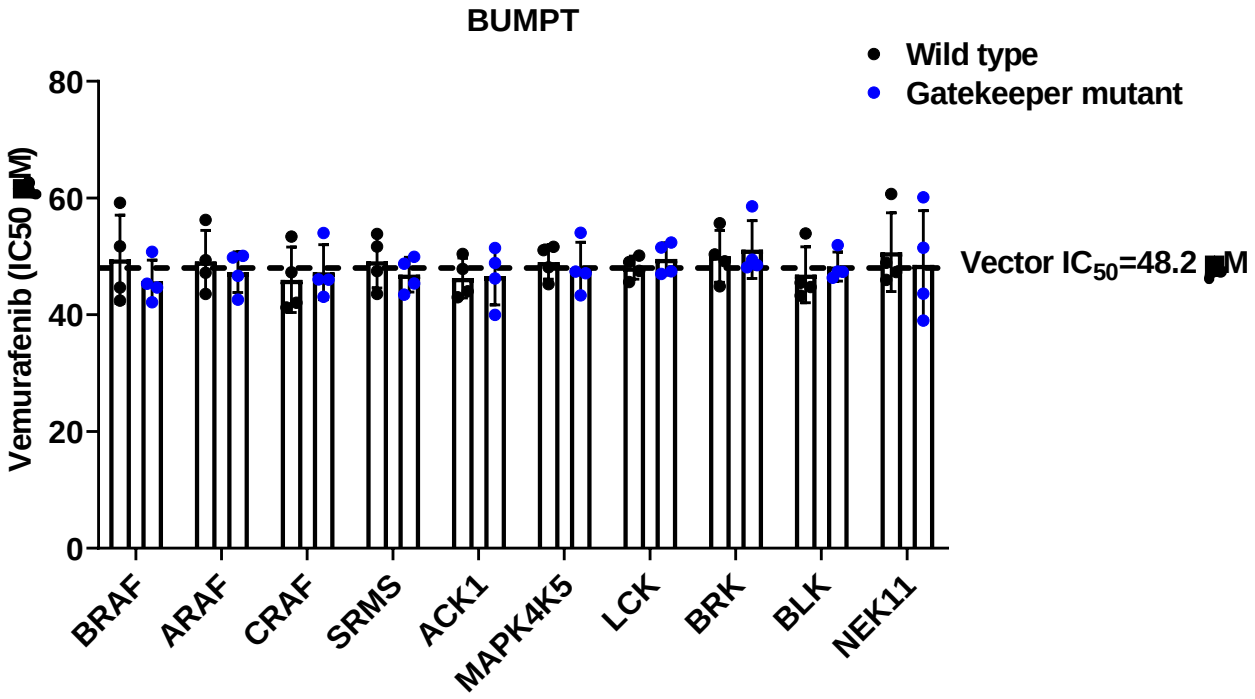

Suppl. Figure 8: ***Chemical genetics approach to evaluate the role of kinase inhibition in vemurafenib-mediated RTEC cell death***. BUMPT cells were transiently transfected with empty vector, wild type or gatekeeper mutants of indicated kinases. One day after transfection, the cells were treated with 0-100 µM vemurafenib, followed by cell viability assessment at 48 hours using trypan blue staining. IC50 (half-maximal inhibitory concentration) was calculated by nonlinear regression analysis. The graph represents data from four independent experiments (n=4 biologically independent samples), experimental values are presented as mean ± s.d. The height of error bar = 1 s.d. and $p < 0.05$ was indicated as statistically significant. One-way ANOVA followed by Dunnett's was carried out and statistical significance is indicated by *$p < 0.05$, **$p < 0.01$, ***$p < 0.001$. The results indicate that none of the tested kinases are involved in vemurafenib-associated RTEC cell death.

Suppl. Figure 9

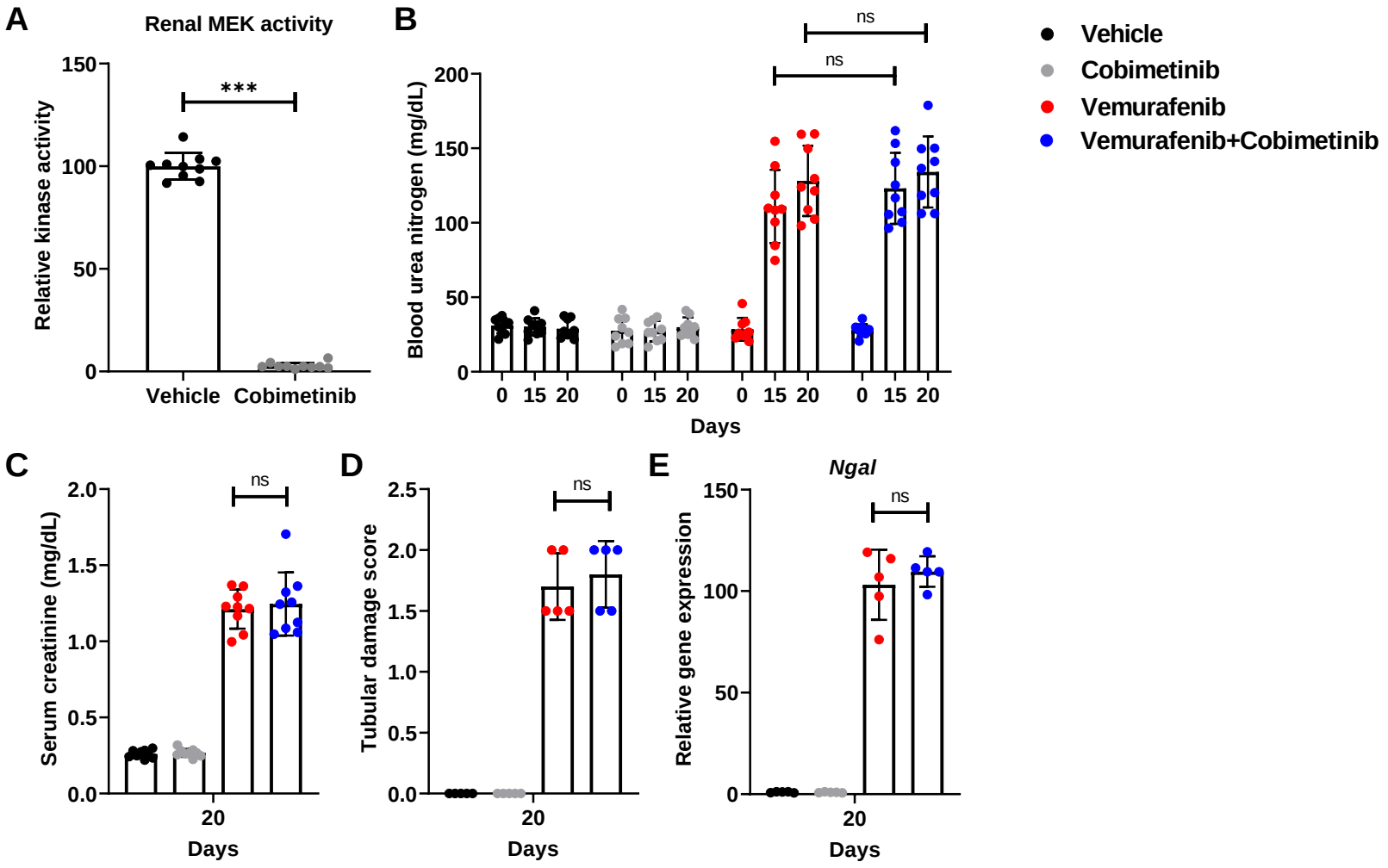

Suppl. Figure 9: ***MEK inhibition does not influence the severity of vemurafenib nephrotoxicity*****. (A)** Age-matched, 8-12 weeks old male C57BL/6J mice were treated with either vehicle or 5 mg/kg cobimetinib (p.o, q.d) for 3 days followed by assessment of renal MEK activity. Under these dosing conditions, a robust inhibition of MEK activity was obtained. (**B-E**) Age-matched, 8-12 weeks old male C57BL/6J mice were treated with either vehicle, 5 mg/kg cobimetinib (p.o, q.d) alone, 20 mg/kg vemurafenib (p.o, b.i.d.) alone or vemurafenib+cobimetinib for 20 days followed by cessation of drug administration for 2 days and subsequent endpoint analysis of renal function. These studies showed that cobimetinib did not influence the severity of vemurafenib nephrotoxicity. In all the bar graphs (n=5-10 biologically independent samples), experimental values are presented as mean ± s.d. The height of error bar = 1 s.d. and $p < 0.05$ was indicated as statistically significant. Student's t-test or non-parametric Mann–Whitney U test was carried out and statistical significance is indicated by *$p < 0.05$, **$p < 0.01$, ***$p < 0.001$.

Suppl. Figure 10

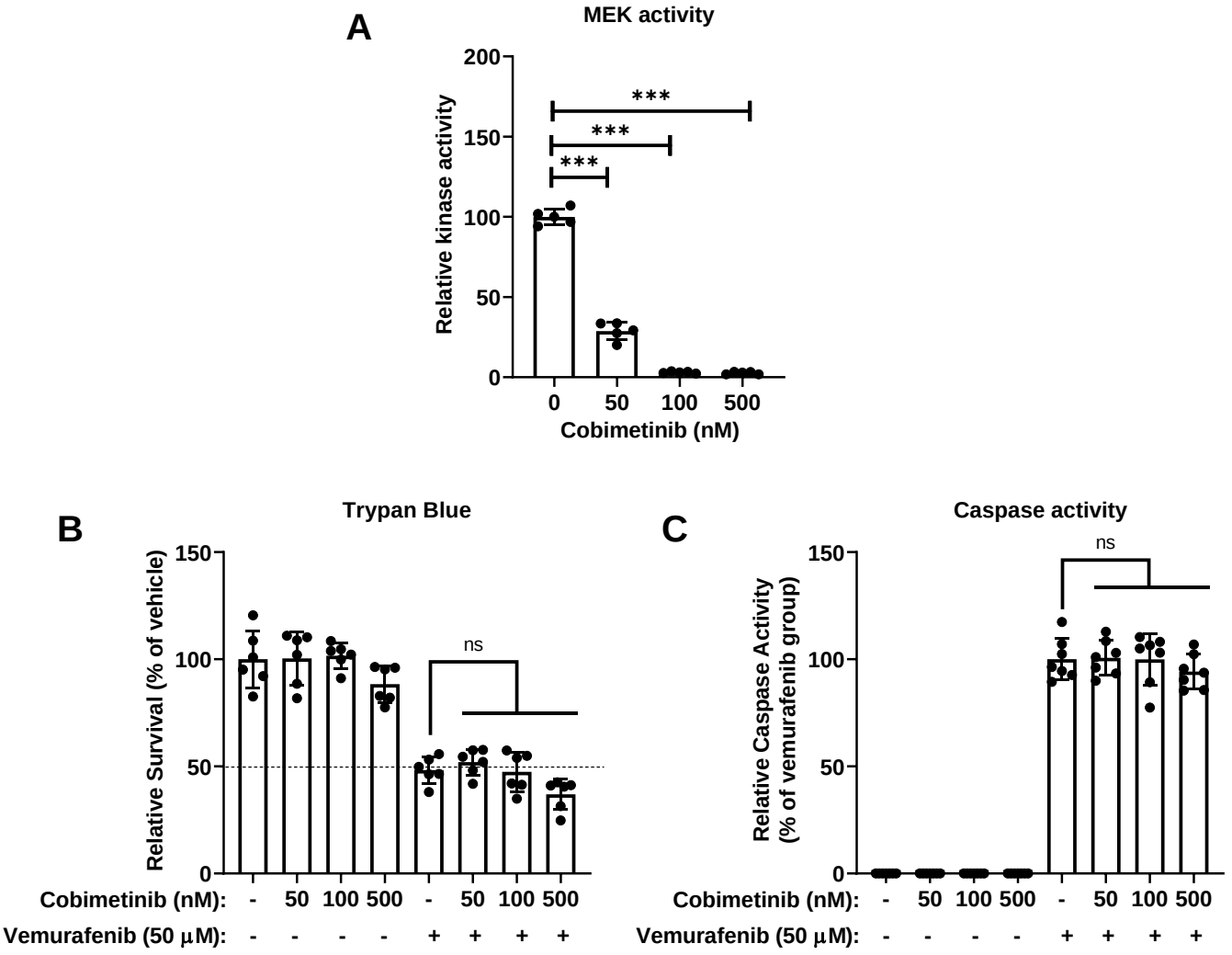

Suppl. Figure 10: ***MEK inhibition does not influence the severity of vemurafenib-induced RTEC cell death*****. (A)** Human RTEC cell line, HK-2 cells were treated with cobimetinib for 24 hours, followed by assessment of MEK kinase activity. These results showed a clear dose-dependent inhibition of MEK kinase activity. **(B-C)** HK-2 cells were co-treated with vemurafenib and cobimetinib for 48 hours followed by assessment of cellular viability and caspase activation. The results indicate that cobimetinib does not influence the severity of vemurafenib-mediated RTEC cell death. In all the bar graphs (n=5-7 biologically independent samples), experimental values are presented as mean ± s.d. The height of error bar = 1 s.d. and $p < 0.05$ was indicated as statistically significant. One-way ANOVA followed by Dunnett's was carried out and statistical significance is indicated by *$p < 0.05$, **$p < 0.01$, ***$p < 0.001$.

Suppl. Figure 11

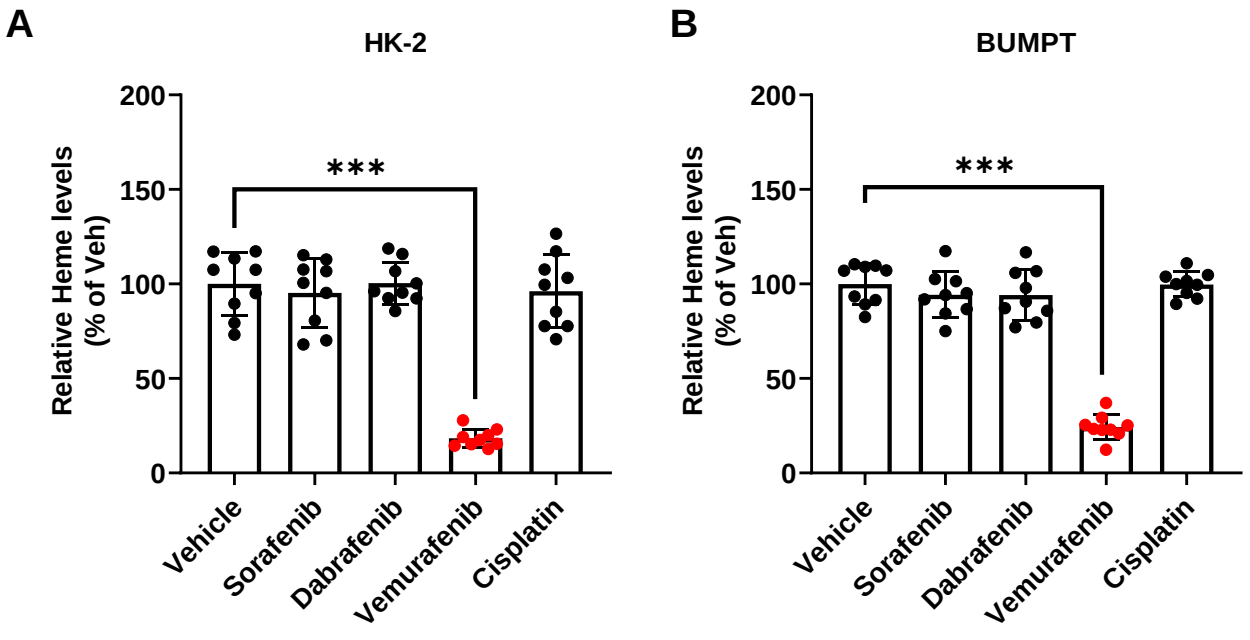

Suppl. Figure 11: ***Vemurafenib induces intracellular heme depletion in RTECs.*** **(A-B)** Tubular epithelial cell lines of murine (BUMPT) and human (HK-2) origin were treated with vehicle, cisplatin or kinase inhibitors including vemurafenib at 50 μM concentration, followed by assessment of intracellular heme levels at 24 hours. In all the bar graphs (n=9 biologically independent samples), experimental values are presented as mean ± s.d. The height of error bar = 1 s.d. and $p < 0.05$ was indicated as statistically significant. One-way ANOVA followed by Dunnett's was carried out and statistical significance is indicated by *p < 0.05, **p < 0.01, ***p < 0.001.

Suppl. Figure 12

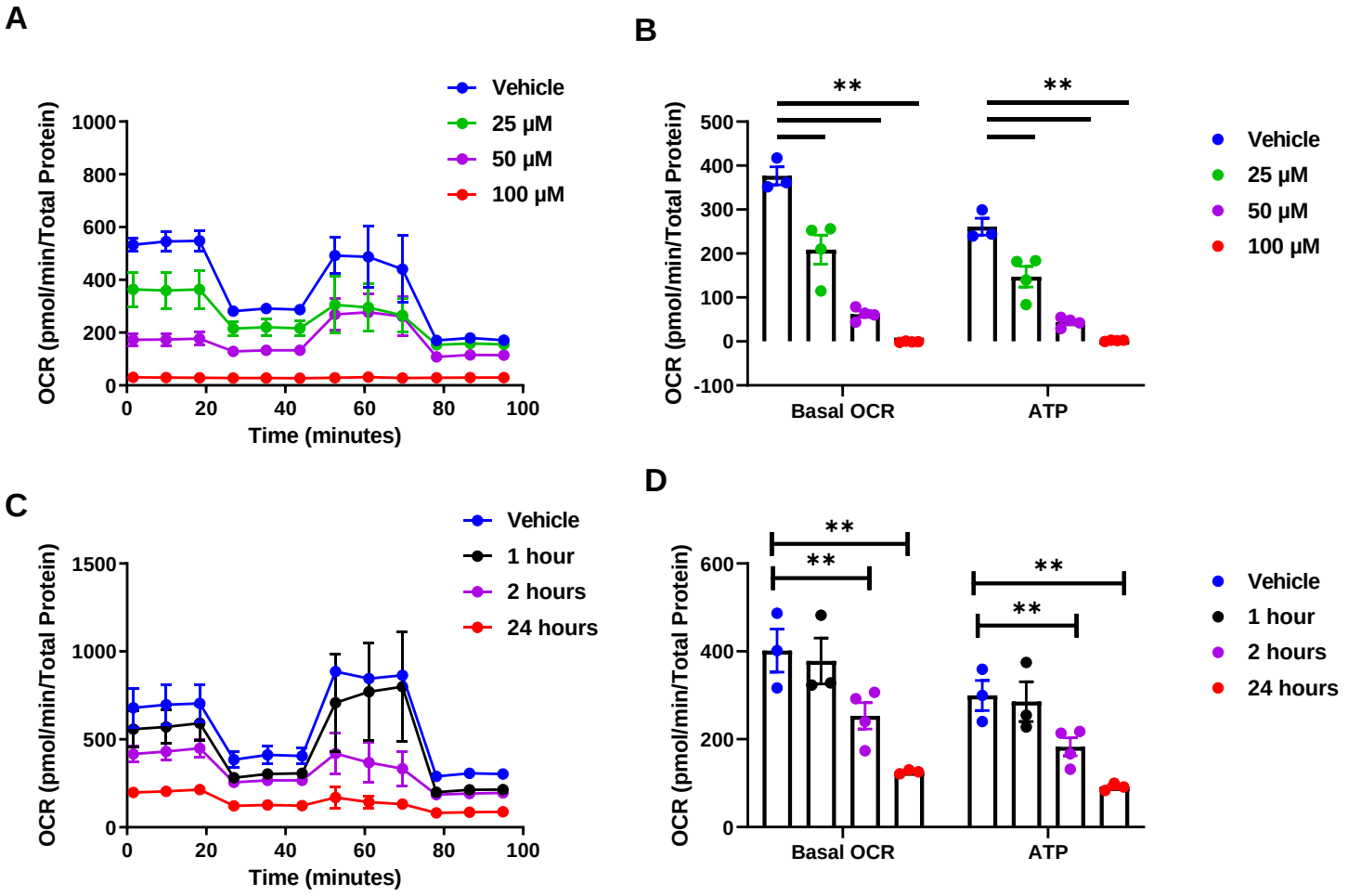

Suppl. Figure 12: ***Vemurafenib induces mitochondrial dysfunction in RTECs.*** **(A-B)** BUMPT cells were seeded in a Seahorse XF-24e analyzer, treated with vehicle or vemurafenib (dose response) for 24 h, and oxygen consumption rate (OCR) was determined during sequential treatments with oligomycin, FCCP and antimycin A/rotenone**.** The graph depicts the quantification of basal oxygen consumption rate (OCR) and ATP production**. (C-D)** BUMPT cells were seeded in a Seahorse XF-24e analyzer, treated with vehicle or 50 µM vemurafenib (time course) for 1-24 h, and oxygen consumption rate (OCR) was determined during sequential treatments with oligomycin, FCCP and antimycin A/rotenone**.** The graph shows the quantification of basal oxygen consumption rate (OCR) and ATP production**.** In all the bar graphs (n=3-4 biologically independent samples), experimental values are presented as mean ± s.d. This experiment was repeated three time and yielded similar results. The height of error bar = 1 s.d. and $p < 0.05$ was indicated as statistically significant. One-way ANOVA followed by Dunnett's was carried out and statistical significance is indicated by *p < 0.05, **p < 0.01, ***p < 0.001.

Suppl. Figure 13

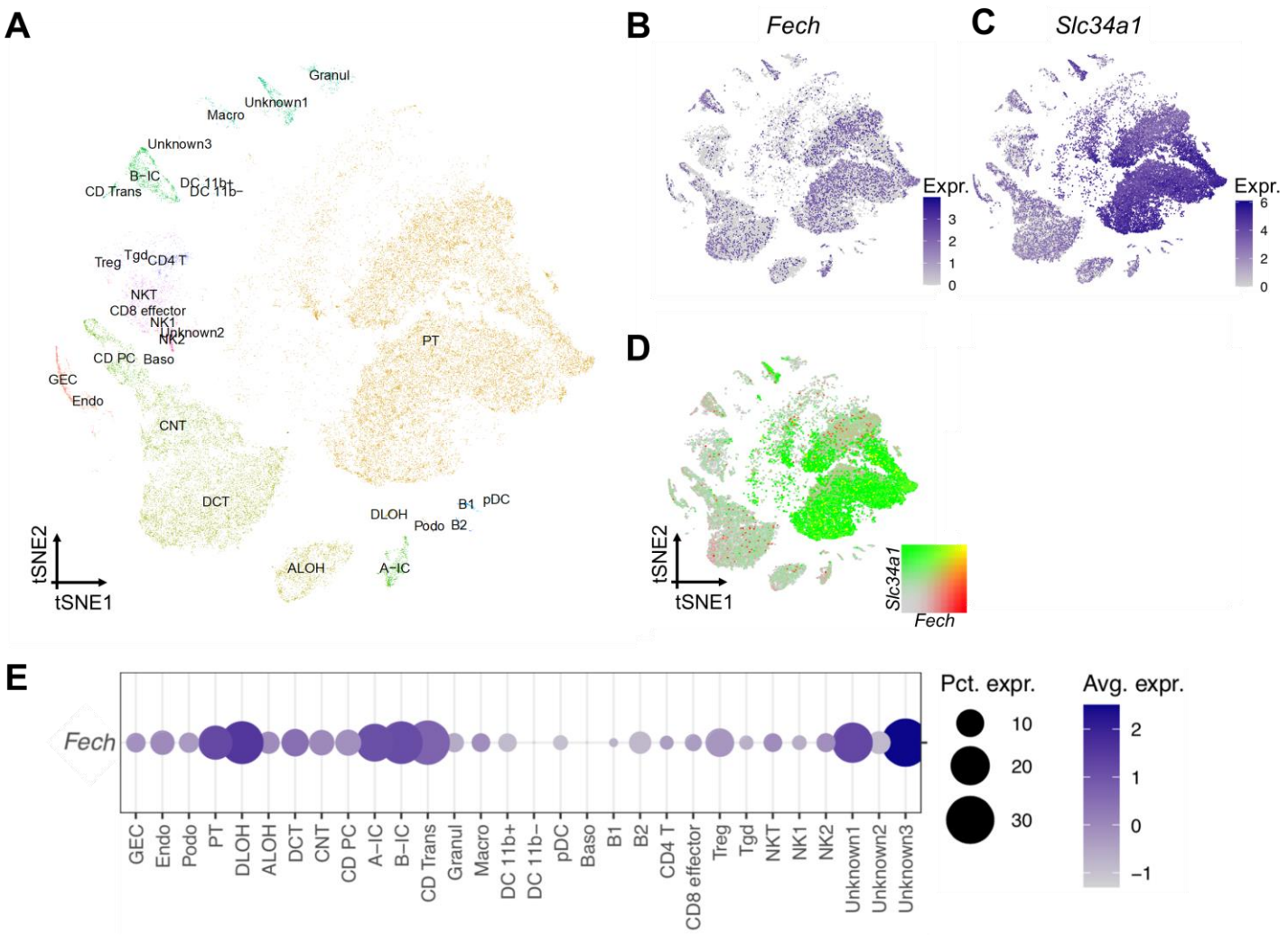

Suppl. Figure 13. ***Fech expression in proximal tubular and other cells of healthy mouse kidneys***. (**A**) Visualization of n=37,361 healthy control kidney cells (*Dhillon et al. 2021*) in t-distributed stochastic neighbor embedding (tSNE) dimension space. GEC, glomerular endothelial cells; Endo, endothelial; Podo, podocyte; PT, proximal tubule; DLOH, descending loop of Henle; ALOH, ascending loop of Henle; DCT, distal convoluted tubule; CNT, connecting tubule; CD-PC, collecting duct principal cell; A-IC, alpha intercalated cell; B-IC, beta intercalated cell; CD-trans. collecting duct transitional cell; Granul, granulocyte; Macro, macrophage; DC 11b+, CD11b+ dendritic cell; pDC, plasmacytoid DC; Baso, basophile; B, B lymphocyte; Treg, regulatory T cell; Tgd, gamma delta T cell; NK, natural killer cell. (**B-D**) Corresponding feature plots for *Fech*, PT marker gene *Slc34a1* and their co-expression. Color represents gene expression. (**E**) Corresponding dot plot for *Fech* gene expression by cell cluster. Dot size denotes percent expression, color denotes average expression.

Suppl. Figure 14

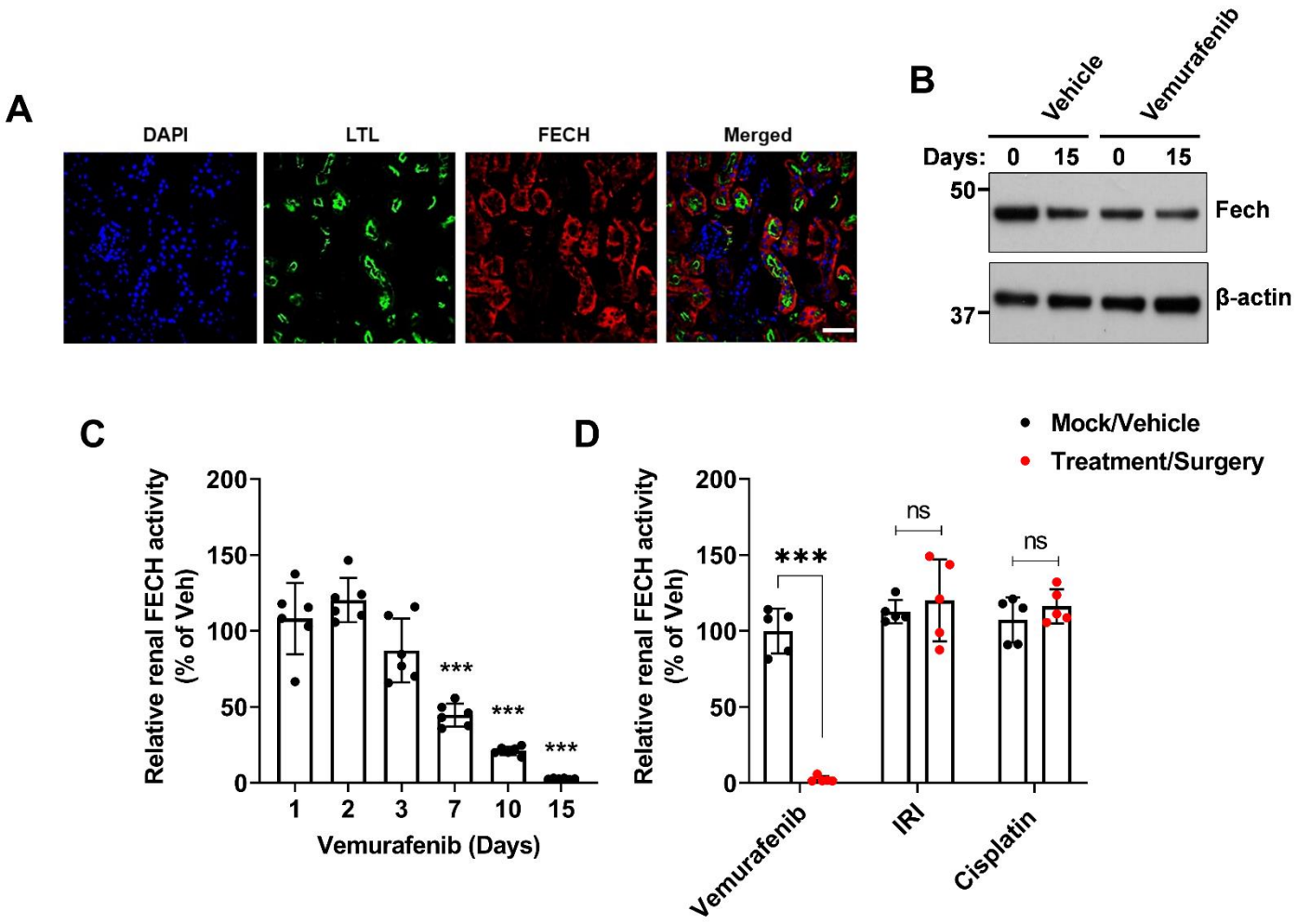

Suppl. Figure 14: ***Vemurafenib associated AKI is associated with renal ferrochelatase inhibition.*** (**A**) Immunofluorescence staining of renal tissues showed high FECH staining in RTECs (LTL positive). Age-matched, 8-12 weeks old male C57BL/6J mice were treated with either vehicle or 20 mg/kg vemurafenib (p.o, b.i.d.) for 15 days. (**B**) Immunoblot analysis of renal FECH expression did not show a significant difference in vehicle and vemurafenib groups. (**C**) Renal FECH assay showed a progressive decline in FECH activity in the vemurafenib treated mice. (**D**) Renal tissues from 8-12 weeks old male C57BL/6J mice treated with 20 mg/kg b.i.d. vemurafenib (15 days), 30 mg/kg cisplatin (day 3) or bilateral renal ischemia (26 minutes followed by 24 hour reperfusion) were used to evaluate renal FECH activity. The results show that reduced in FECH activity during vemurafenib-associated AKI is not an indirect effect of kidney injury. In all the bar graphs (n=5-6 biologically independent samples), experimental values are presented as mean ± s.d. The height of error bar = 1 s.d. and $p < 0.05$ was indicated as statistically significant. Student's t-test (A-I) was carried out and statistical significance is indicated by *$p < 0.05$, **$p < 0.01$, ***$p < 0.001$.

Suppl. Figure 15

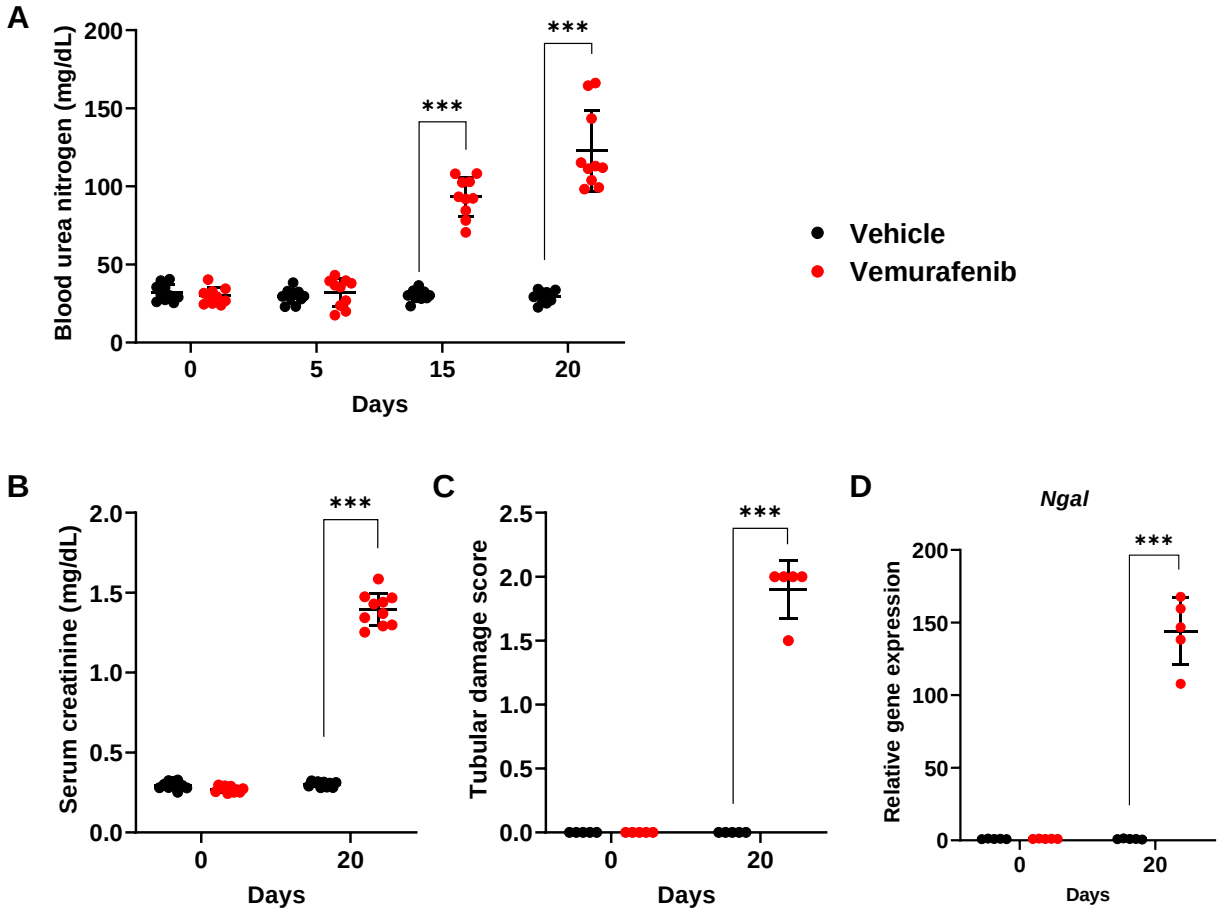

Suppl. Figure 15: ***Vemurafenib nephrotoxicity in the transgenic reporter mice.*** We crossed the Ggt1-Cre mice with ROSAmT/mG mice to generate the transgenic mice that express membrane localized GFP in RTECs. Age-matched, 8-12 weeks old male mice were treated with either vehicle or 20 mg/kg vemurafenib (p.o, b.i.d.) for 20 days followed by cessation of drug administration for 2 days and subsequent endpoint analysis of renal function. (**A**) Blood urea nitrogen levels showed that vemurafenib can induce AKI after 2 weeks of continuous treatment and cessation of drug administration reversed the increase in BUN levels. (**B**) Vemurafenib treatment also resulted in increased serum creatinine levels. (**C**) Histological analysis of renal tissues showed that vemurafenib treated mice had clear tubular epithelial injury and cell death. (**D**) Renal *Ngal* gene expression analysis further confirmed significant renal damage in vemurafenib treated mice. In all the bar graphs (n=5-10 biologically independent samples), experimental values are presented as mean ± s.d. The height of error bar = 1 s.d. and $p < 0.05$ was indicated as statistically significant. Student's t-test or non-parametric Mann–Whitney U test was carried out and statistical significance is indicated by *p < 0.05, **p < 0.01, ***p < 0.001.

Suppl. Figure 16

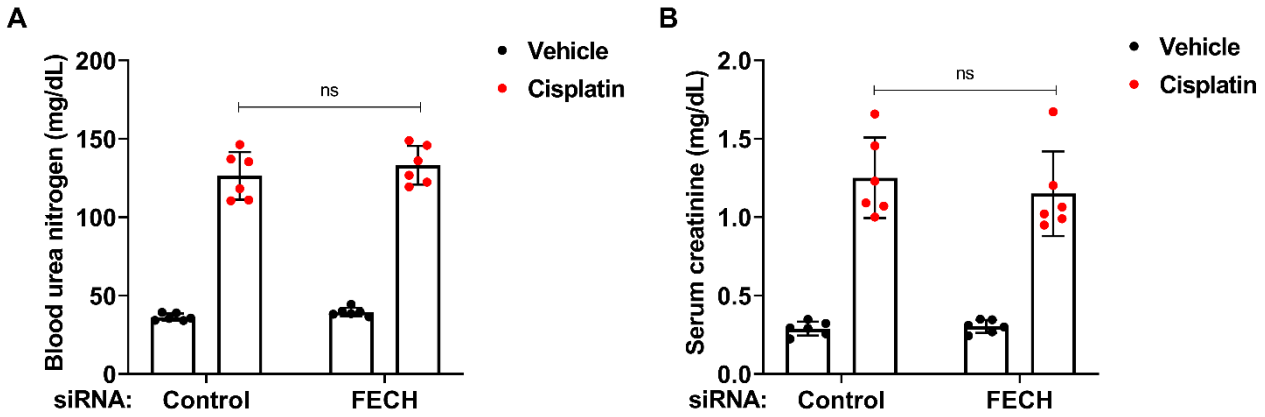

Suppl. Figure 16: ***In vivo siRNA mediated FECH knockdown does not influence the severity of cisplatin nephrotoxicity.*** Age-matched male (8-12 weeks) C57BL/6 mice were administered with three once-daily intravenous injections (hydrodynamic) of control (non-specific) or FECH targeting siRNAs (25 µg in 0.5 ml of PBS). One day later mice were treated with either vehicle or 30 mg/kg cisplatin (i.p.), followed by endpoint analysis of renal function at day 3. (**A**) Blood urea nitrogen, (**B**) serum creatinine measurement showed that the FECH knockdown did not alter the severity of cisplatin nephrotoxicity. In all the bar graphs (n=6 biologically independent samples), experimental values are presented as mean ± s.d. The height of error bar = 1 s.d. and $p < 0.05$ was indicated as statistically significant. One-way ANOVA followed by Tukey's multiple-comparison test was carried out and statistical significance is indicated by *$p < 0.05$, **$p < 0.01$, ***$p < 0.001$.

Suppl. Figure 17

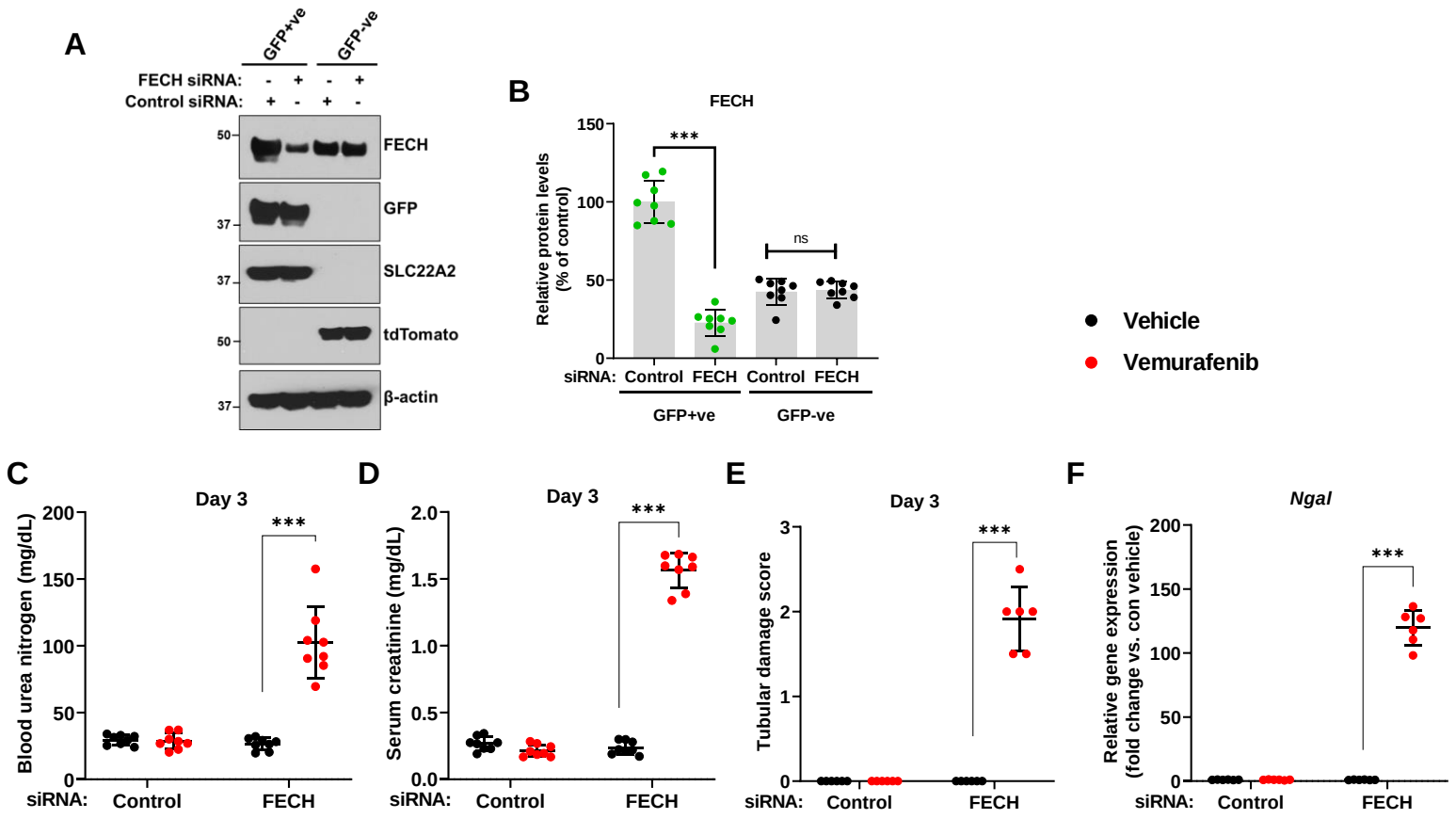

Suppl. Figure 17: ***In vivo siRNA mediated FECH knockdown in reporter mice.*** We crossed the Ggt1-Cre mice with ROSAmT/mG mice to generate the transgenic mice that express membrane localized GFP in RTECs. (**A-B**) Age-matched male (8-12 weeks) were administered with three once-daily intravenous injections (hydrodynamic) of control (non-specific) or FECH targeting siRNAs (25 µg in 0.5 ml of PBS). Three days later, the mice were euthanized, kidneys were excised and GFP positive and negative cells were isolated. Immunoblot analysis of these cells showed that FECH knockdown occurred only in the GFP positive (RTEC) cells. (**C-F**) Age-matched male (8-12 weeks) mice were administered with three once-daily intravenous injections (hydrodynamic) of control (non-specific) or FECH targeting siRNAs (25 µg in 0.5 ml of PBS). One day later mice were treated with either vehicle or 20 mg/kg vemurafenib (p.o, b.i.d.) for 3 days followed by endpoint analysis of renal function. Blood urea nitrogen, serum creatinine, histological examination, and renal *Ngal* expression analysis showed that the FECH knockdown mice developed vemurafenib nephrotoxicity within 3 days of treatment, while the control group demonstrated no obvious renal injury or damage. In all the bar graphs (n=6-8 biologically independent samples), experimental values are presented as mean ± s.d. The height of error bar = 1 s.d. and $p < 0.05$ was indicated as statistically significant. One-way ANOVA followed by Tukey's multiple-comparison test or non-parametric Mann–Whitney U test was carried out and statistical significance is indicated by *$p < 0.05$, **$p < 0.01$, ***$p < 0.001$.

Suppl. Figure 18

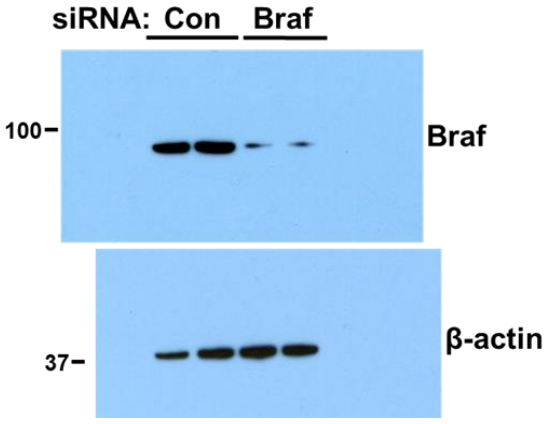

Figure 1E

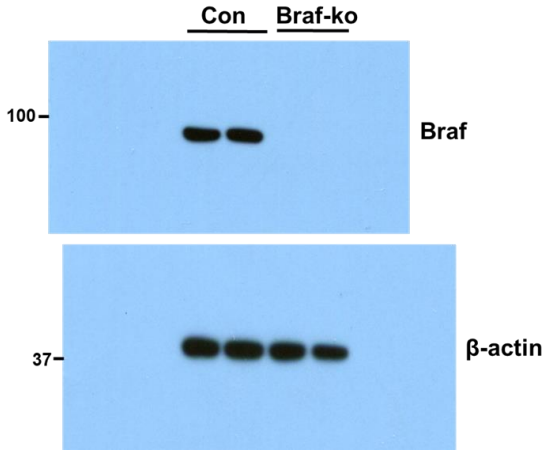

Figure 1F

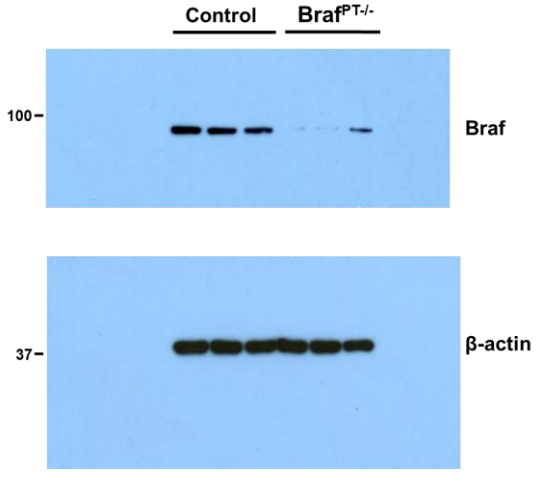

Figure 3B

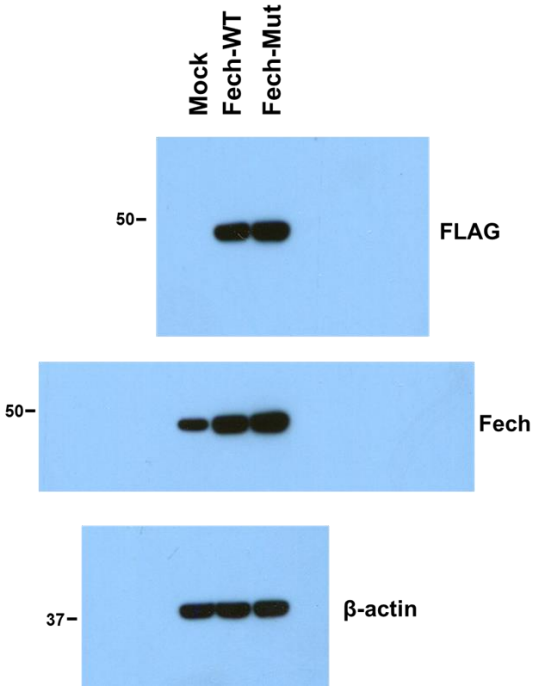

Figure 4C

Suppl. Figure 18: ***Uncropped images of immunoblot data.***

Suppl. Figure 18 (continued)

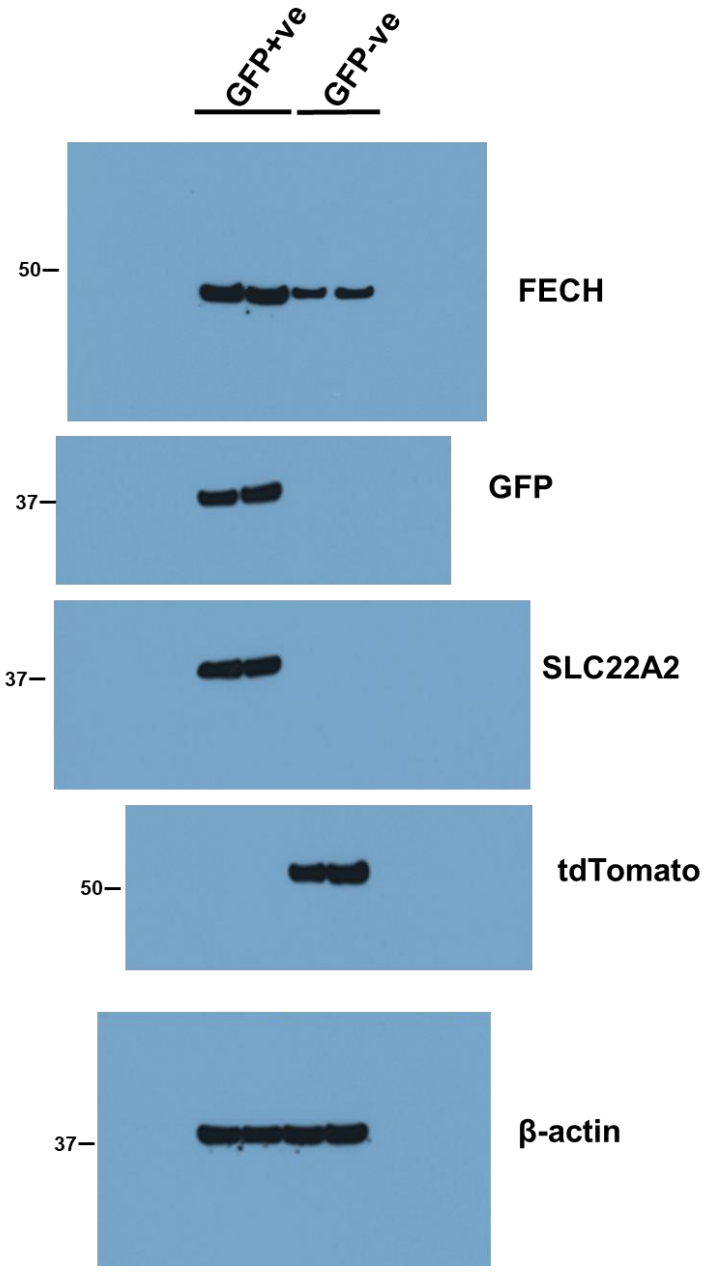

Figure 5D

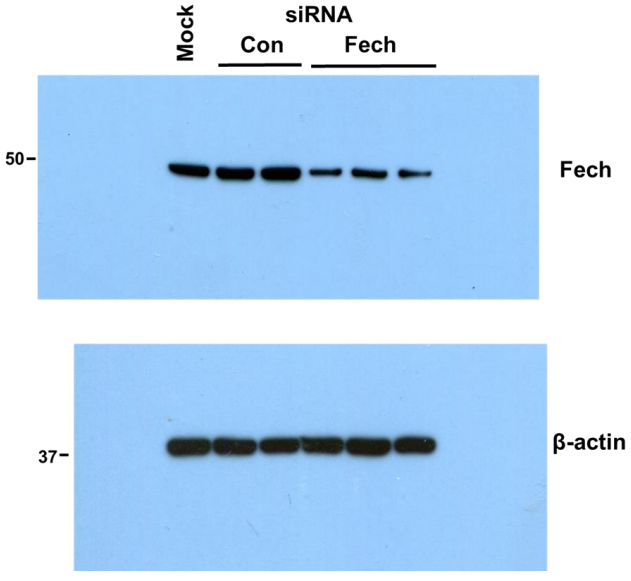

Figure 6A

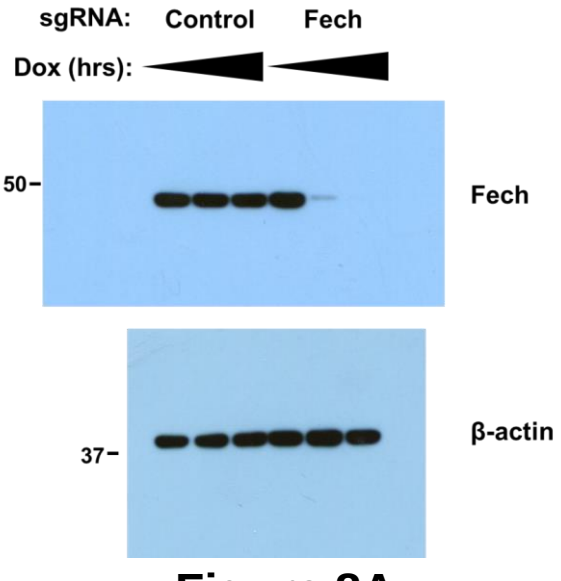

Figure 8A

Suppl. Figure 18: ***Uncropped images of immunoblot data (continued).***

Suppl. Figure 18 (continued)

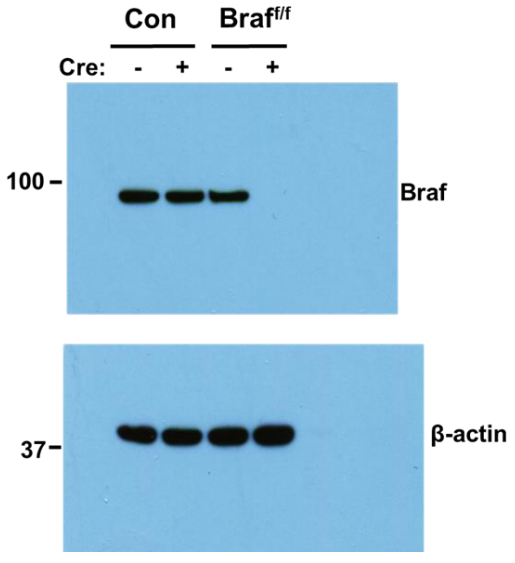

Suppl. Figure 7A

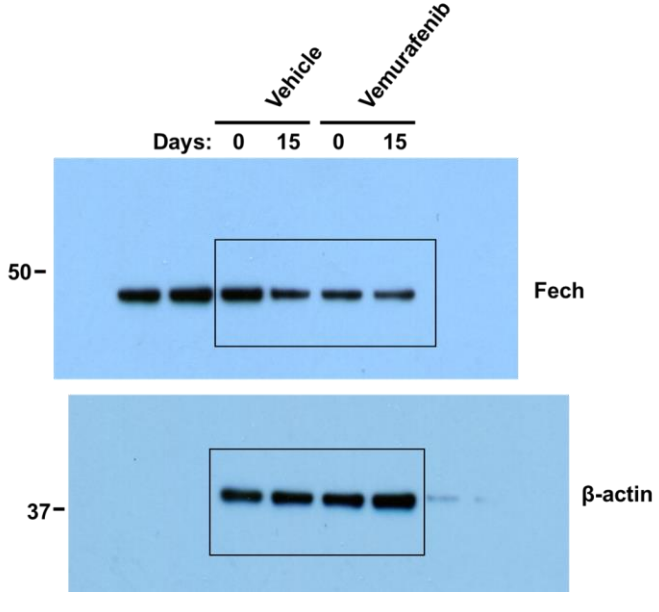

Suppl. Figure 14B

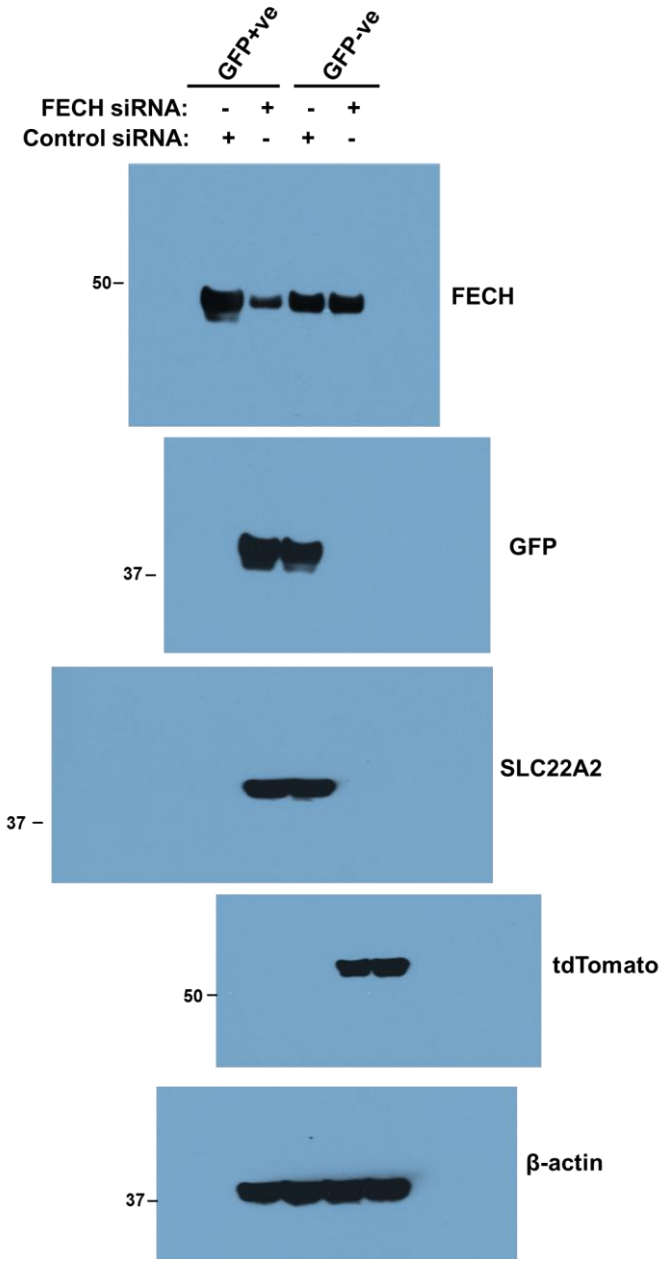

Suppl. Figure 17A

Suppl. Figure 18: ***Uncropped images of immunoblot data (continued).***